Sam68 regulates translation of target mRNAs in male germ cells, necessary for mouse spermatogenesis

Maria Paola Paronetto,[1,3] Valeria Messina,[1,3] Enrica Bianchi,[1,3] Marco Barchi,[1] Gillian Vogel,[5,6,7] Costanzo Moretti,[2] Fioretta Palombi,[4] Mario Stefanini,[4] Raffaele Geremia,[1] Stéphane Richard,[5,6,7] and Claudio Sette[1,3]

[1]Department of Public Health and Cell Biology, Section of Anatomy, and [2]Department of Internal Medicine, University of Rome Tor Vergata, 00133 Rome, Italy
[3]Laboratory of Neuroembryology, Fondazione Santa Lucia, 00143 Rome, Italy
[4]Department of Histology and Medical Embryology, Università di Roma La Sapienza, 00110 Rome, Italy
[5]Terry Fox Molecular Oncology Group and the Bloomfield Center for Research on Aging, Lady Davis Institute for Medical Research, Sir Mortimer B. Davis Jewish General Hospital, [6]Department of Oncology, and [7]Department of Medicine, McGill University, Montréal, Québec, Canada, H3T1E2

Sam68 is a KH-type RNA-binding protein involved in several steps of RNA metabolism with potential implications in cell differentiation and cancer. However, its physiological roles are still poorly understood. Herein, we show that *Sam68*$^{-/-}$ male mice are infertile and display several defects in spermatogenesis, demonstrating an essential role for Sam68 in male fertility. *Sam68*$^{-/-}$ mice produce few spermatozoa, which display dramatic motility defects and are unable to fertilize eggs. Expression of a subset of messenger mRNAs (mRNAs) is affected in the testis of knockout mice. Interestingly, Sam68 is associated with polyadenylated mRNAs in the cytoplasm during the meiotic divisions and in round spermatids, when it interacts with the translational machinery. We show that Sam68 is required for polysomal recruitment of specific mRNAs and for accumulation of the corresponding proteins in germ cells and in a heterologous system. These observations demonstrate a novel role for Sam68 in mRNA translation and highlight its essential requirement for the development of a functional male gamete.

Introduction

Mammalian spermatogenesis is a striking example of posttranscriptional regulation of gene expression (Schafer, et al., 1995; Braun 1998; Walker et al., 1999; Elliott, 2003). Because de novo transcription is not always possible during germ cell differentiation, the mRNAs for several proteins involved in spermatogenesis need to be synthesized and stored well before their translation is needed. Chromatin becomes unavailable for transcription during homologous recombination in the first meiotic prophase (Turner, et al., 2005). It follows a wave of intense transcription at the pachytene stage until the onset of chromatin condensation that precedes the first division (Monesi, 1964). Later, when round spermatids differentiate into elongated spermatozoa, the nucleus is rendered transcriptionally inactive due to extensive nuclear remodeling, replacement of histones with the highly basic protamines, and compaction of the chromatin (Sassone-Corsi, 2002). As a consequence of these processes, several mRNAs synthesized during the transcriptionally active stages of spermatogenesis are stored and protected by a profusion of ribonucleoproteins (RNPs), which preserve them until their translation begins (Geremia, et al., 1977; Schafer et al., 1995; Kleene, 2001). In particular, it was found that >700 transcripts are differentially shifted from the RNPs to the polysomes in a developmentally regulated manner during spermatogenesis (Iguchi et al., 2006). However, the mechanisms and the RNA-binding proteins (RBPs) that participate to their translational control in male germ cells are still largely unknown.

Correspondence to Claudio Sette: claudio.sette@uniroma2.it; or Stéphane Richard: Stephane.Richard@mcgill.ca

Maria Paola Paronetto's present address is Centre de Regulaciò Genomica, Barcelona 08003, Spain.

Abbreviations used in this paper: ANOVA, analysis of variance; dpp, days postpartum; ERK, extracellular signal-regulated kinase; IPA, Ingenuity Pathway Analysis; OA, okadaic acid; RBP, RNA-binding protein; RNP, ribonucleoprotein; STAR, signal transduction and activation of RNA; UTR, untranslated region.

The Rockefeller University Press $30.00
J. Cell Biol. Vol. 185 No. 2 235–249
www.jcb.org/cgi/doi/10.1083/jcb.200811138

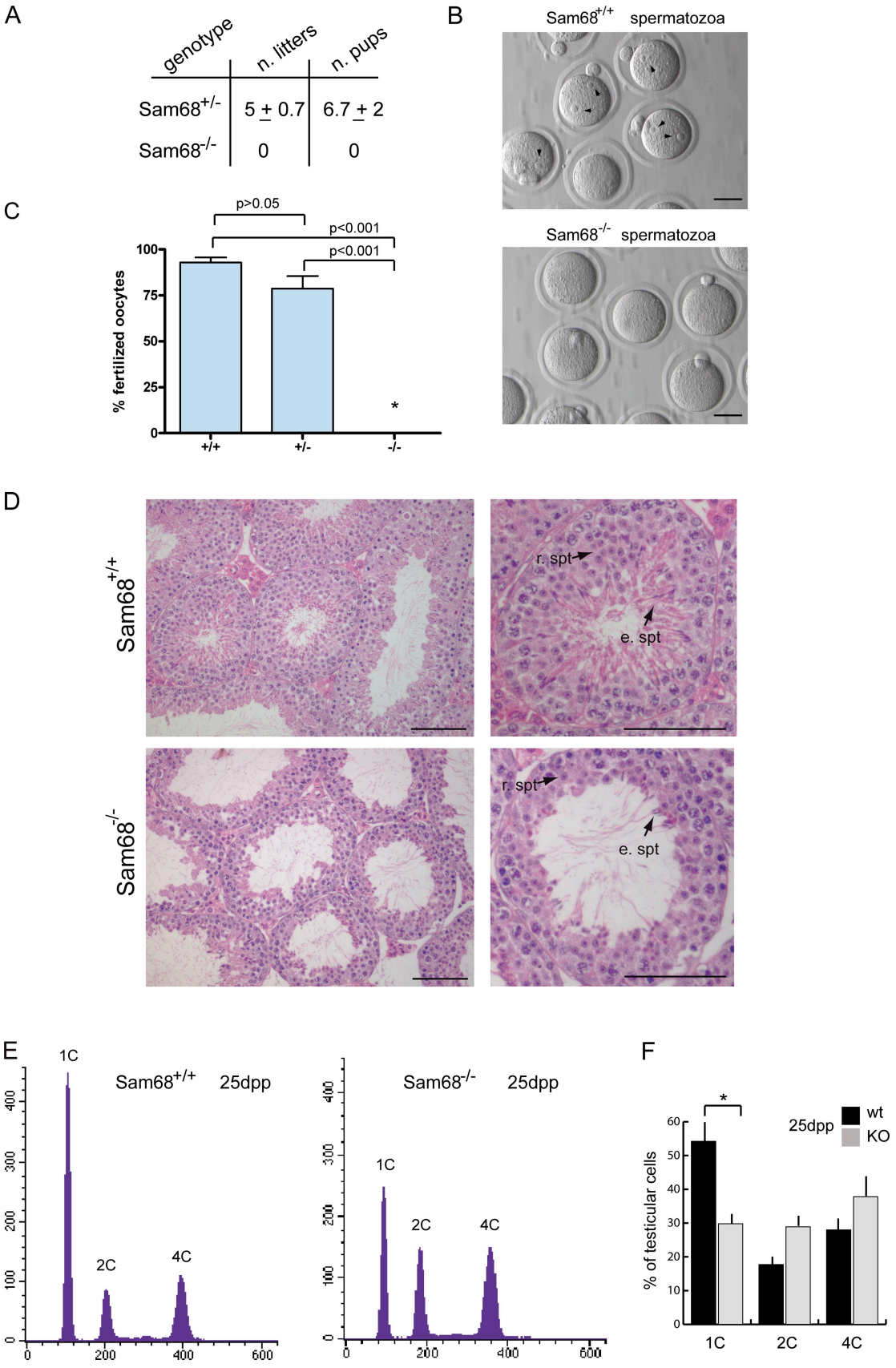

Figure 1. **Sam68 is required for male fertility.** (A) Analysis of the fertility phenotype of *Sam68*$^{+/-}$ (n = 5) and *Sam68*$^{-/-}$ (n = 6) mice. Mice were bred for 5 mo with wild-type females of proven fertility. Females were changed each time they remained pregnant or after 2.5 mo without remaining pregnant. (B and C) Ovulation was induced in wild-type females by hormonal treatment before mating with *Sam68*$^{+/+}$ (n = 3), *Sam68*$^{+/-}$ (n = 3), and *Sam68*$^{-/-}$ (n = 3) males. Mating was confirmed by observation of the vaginal plug 15 h later, and oocytes were collected from the oviducts 18 h after mating. Fertilization

A class of RBPs that play essential roles in development is represented by the signal transduction and activation of RNA (STAR) family (Lukong and Richard, 2003; Volk et al., 2008). A prototype STAR protein, the *Caenorhabditis elegans* GLD-1, functions as translational regulator during female gametogenesis (Francis, et al., 1995, Lee and Schedl, 2001). The mammalian STAR protein QUAKING (QKI) has been shown to regulate mRNA stability, mRNA export, and pre-mRNA splicing (Chenard and Richard 2008; Volk et al., 2008). Another mammalian STAR protein, Src-associated substrate in mitosis of 68 kD (Sam68 or KHDRBS1; Fumagalli et al., 1994; Taylor and Shalloway, 1994), plays a role in several aspects of RNA metabolism, from alternative splicing (Matter et al., 2002, Cheng and Sharp, 2006; Paronetto, et al., 2007; Chawla et al., 2009) to nuclear export (Li et al., 2002) and cytoplasmic utilization of viral mRNAs (Coyle, et al., 2003). Moreover, Sam68 was found associated to the polysomes in depolarizing neurons and meiotic germ cells (Grange et al., 2004; Paronetto et al., 2006). Src-related kinases and mitogen-activated kinases phosphorylate Sam68 and regulate its RNA-binding affinity (Wang et al., 1995; Tisserant and König, 2008) and its activity in alternative splicing (Matter et al., 2002; Paronetto et al., 2007), which indicates that Sam68 is able to integrate intracellular signals and RNA processing. Mice with knockout for the *Sam68* gene are protected from age-related bone loss and mammary gland tumors, revealing a function of this protein in mesenchymal stem cell differentiation (Richard, et al., 2005), tumorigenesis, and metastasis (Lukong et al., 2008; Richard et al., 2008). Nevertheless, whether or not the defects observed in *Sam68*$^{-/-}$ mice are caused by deregulation of specific cellular mRNAs in the cell remains unknown.

In this paper, we show that male *Sam68* knockout mice are infertile due to aberrant differentiation of round spermatids into mature spermatozoa. We have identified a subset of testicular transcripts that are affected by Sam68 ablation and found an enrichment in mRNAs encoding proteins involved in cell proliferation and survival. Several of these mRNAs are bound by Sam68 in germ cells. Moreover, we provide evidence that upon meiotic divisions, Sam68 associates with the translation initiation complex and regulates polysomal loading and translation of the mRNAs encoding SPAG16, a cytoskeletal protein required for sperm motility and fertility; NEDD1, a centrosomal protein required for microtubule organization; and SPDYA, a cell cycle regulator. Our findings suggest that *Sam68* loss of function leads to male infertility by restricting translation of a selected group of mRNA transcripts.

Results

Sam68 is required for male fertility

Sam68 expression is strongly expressed in meiotic and postmeiotic male germ cells of the testis, which suggests a role in spermatogenesis (Fig. S1). To investigate whether Sam68 is required for male fertility, we analyzed the reproductive phenotype of *Sam68*$^{-/-}$ mice. Crosses with wild-type females of proven fertility indicated that *Sam68*$^{-/-}$ males did not produce offspring, whereas *Sam68*$^{+/-}$ males were fertile (Fig. 1 A). To rule out behavioral defects affecting mating, *Sam68*$^{+/+}$, *Sam68*$^{+/-}$, or *Sam68*$^{-/-}$ males were crossed with hormonally primed wild-type females, and mating was scored by observation of the vaginal plug. Although *Sam68*$^{-/-}$ mice formed plugs, they were unable to fertilize wild-type oocytes, as shown by the lack of pronuclei (Fig. 1, B and C), whereas their littermates were fertile in this assay. These findings show that Sam68 expression is required for male fertility and that the infertile phenotype of *Sam68*$^{-/-}$ males is not due to altered mating behavior.

Sam68 expression is required for the correct progression of spermatogenesis

Testicular atrophy is a common feature of infertile knockout male mice. Although Sam68 depletion did not cause general testicular atrophy, the testis/body weight ratio was significantly lower in *Sam68*$^{-/-}$ as compared with their littermate controls (Fig. S2, A–C). Serum testosterone levels, although very variable from animal to animal, were not significantly different in *Sam68*$^{-/-}$ mice (Fig. S2, D), which indicates that the smaller testis size and male infertility were not caused by decreased androgen levels. The seminiferous tubules of adult *Sam68*$^{-/-}$ mice had a thinner epithelium than the wild-type tubules due to a strong reduction in postmeiotic haploid cells, which affected both the early round spermatids and the more differentiated elongated spermatids (Fig. 1 D). A developmental analysis of testicular histology revealed that the defects in spermatogenesis of *Sam68*$^{-/-}$ mice first appeared at the time when the bulk of meiotic divisions occurs (25 days postpartum [dpp] in Fig. S3). The reduction in postmeiotic cells was maintained throughout the first spermatogenic wave (45 dpp in Fig. S3). In contrast, no major defects were apparent at 16 dpp, before the onset of the meiotic divisions (Fig. S3). Analysis of DNA content in purified germ cells by flow cytometry quantified the reduction in haploid spermatids of *Sam68*$^{-/-}$ mice to 45% in juvenile (Fig. 1, E and F) and 29% in adult testes (Fig. S2 E).

Aberrant divisions of meiotic cells were observed in *Sam68*$^{-/-}$ testis (Fig. S2, F and G). Histological examination revealed the presence of incompletely divided germ cells, containing two or three nuclei of postmeiotic round spermatids that were prematurely shed in the lumen of the tubule (Fig. S2 G). Moreover, TUNEL assays showed the presence of a larger number of dying germ cells in *Sam68*$^{-/-}$ testes, especially at 25 dpp, when most tubules contain meiotically dividing spermatocytes or early round spermatids (Fig. 2 A). Flow cytometry showed that increased apoptosis affected all germ cells in 25-dpp animals (Fig. 2, B and C).

was scored by monitoring formation of the pronuclei (indicated by arrowheads in B) in the fertilized eggs. A graph showing the results of three independent mating experiments is shown in C. Data are represented as the mean ± SD; knockout spermatozoa never fertilized oocytes; SD = 0 in three experiments. *, $P = 9.45 \times 10^{-8}$ in the *t* test; ANOVA test yielded $P < 0.001$. (D) Histological analysis of testis from adult mice. Low (left) and high magnification (right) are shown. Arrows indicate round spermatids (r. spt) and elongated spermatids (e. spt) that are dramatically decreased in the Sam68 knockout testis. (E) Profile of propidium iodide–stained purified germ cells from testes of Sam68 wild-type or knockout mice at 25 dpp of age. Peaks corresponding to 1C, 2C, or 4C DNA content are indicated. Quantitative data of the percentage of each germ cell type from three independent experiments are shown in F (data are represented as mean ± SEM). *, $P < 0.01$ in a *t* test. Bars: (B) 50 µm; (D) 100 µm.

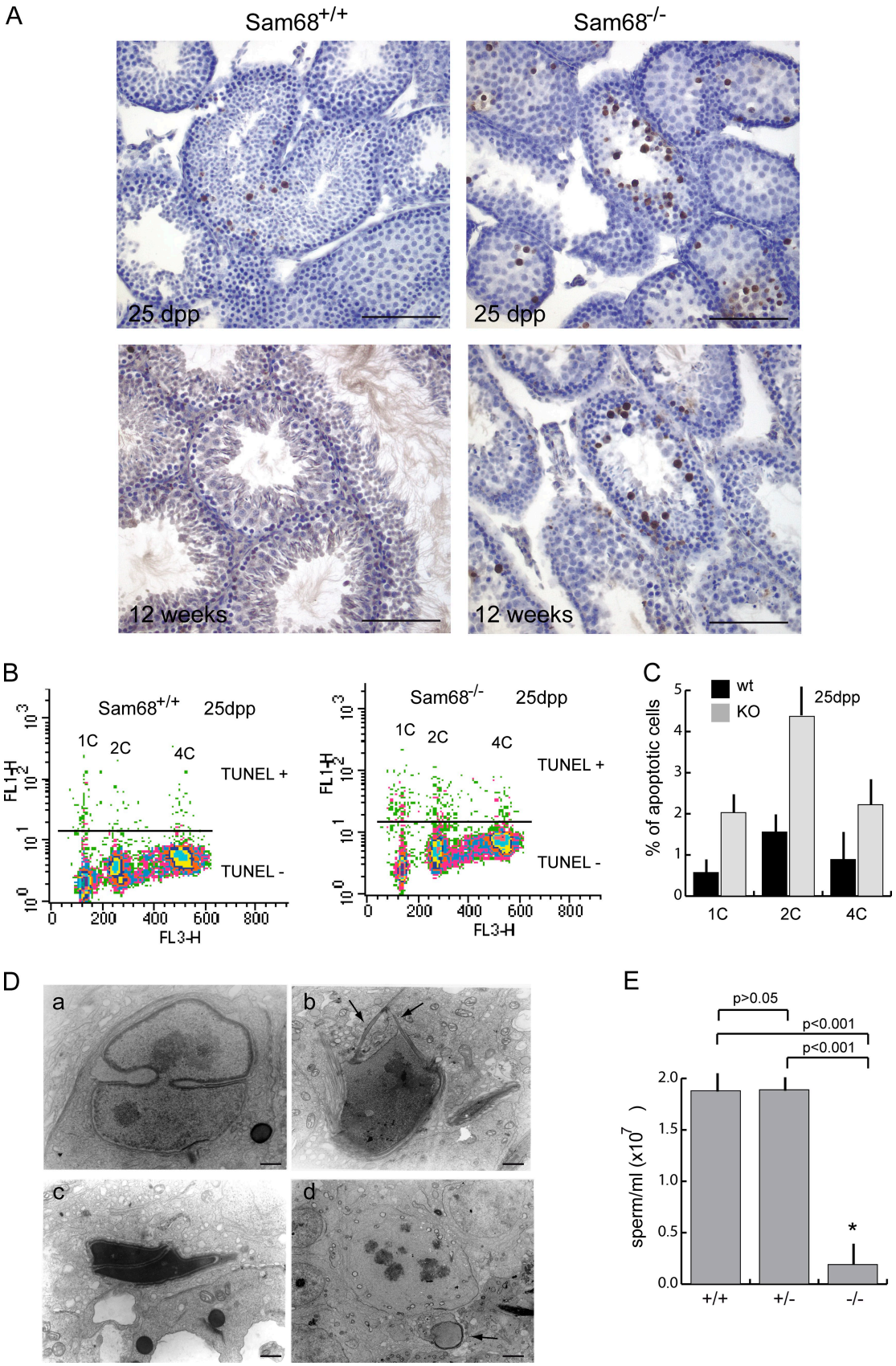

Figure 2. **Ablation of Sam68 increases germ cell apoptosis and impairs spermiogenesis.** (A) TUNEL staining of testicular sections from wild-type or knockout 25 dpp (top) and adult (bottom) mice. *Sam68*$^{-/-}$ testes show increased apoptosis. Nuclear brown signal indicates apoptotic cells. In adult testis, apoptotic cells mainly reside in the luminal pole of the tubule where the haploid cells are localized. Bars, 100 µm. (B) Flow cytometry analysis of TUNEL-positive germ cells. Staining with propidium iodine (x axis) allowed us to identify haploid (1C), diploid (2C), or tetraploid (4C) germ cells. TUNEL staining

Electron microscopy confirmed the severe defects in spermiogenesis in *Sam68*$^{-/-}$ testis. We observed several frequent abnormalities, ranging from aberrant nuclear divisions (Fig. 2 D, a), elongating spermatids with two flagella (Fig. 2 D, b, arrows), elongated spermatids with two nuclei (Fig. 2 D, c), and delayed spermatid differentiation, with step 9–10 spermatids observed in tubules at stage XII (Fig. 2 D, d, arrow). Nevertheless, although they were strongly reduced in number (Fig. 2 E), few mature spermatozoa were found in the epididymis of approximately half of the *Sam68*$^{-/-}$ mice analyzed ($n = 20$). Most of the spermatozoa produced by these *Sam68*$^{-/-}$ mice were abnormally shaped and immotile. Some spermatozoa displayed motility but the majority lost their flagellum shortly after their release in fertilization medium (Video 1). Moreover, the few *Sam68*$^{-/-}$ spermatozoa that maintained reduced motility in culture (Video 2) were completely infertile even under in vitro fertilization conditions (Fig. S2, H and I). These results demonstrate that Sam68 is required for production of male haploid cells and spermiogenesis.

Sam68 ablation affects the expression of a selected number of mRNAs in mouse testis

Although Sam68 is an RBP, it is currently unknown whether its function in vivo requires modulation of specific mRNAs. To investigate this issue, we compared the expression of mRNAs in testes from wild-type and knockout adult mice using the Affymetrix gene expression chips. We found that 294 and 124 targets were significantly ($P < 0.05$) down-regulated and up-regulated in *Sam68*$^{-/-}$ testes (Fig. 3 A; Tables S1 and S2), respectively. Analysis through the Ingenuity Pathway Analysis (IPA) Systems revealed that the top four functional categories among the down-regulated targets were cell cycle ($P = 1.09 \times 10^{-4}$–4.12×10^{-2}), cell death ($P = 1.09 \times 10^{-4}$–4.12×10^{-2}), cancer ($P = 3.24 \times 10^{-4}$–4.12×10^{-2}), and cell-to-cell signaling and interaction ($P = 3.24 \times 10^{-4}$–3.11×10^{-2}; Fig. 3 B; Tables S3 and S4). Regarding the up-regulated targets, the top four functional categories were cell cycle ($P = 5.43 \times 10^{-4}$–4.97×10^{-2}), connective tissue development and function ($P = 5.43 \times 10^{-4}$–4.86×10^{-2}), cell morphology ($P = 7.93 \times 10^{-4}$–3.15×10^{-2}), and nervous system development and function ($P = 7.93 \times 10^{-4}$–4.52×10^{-2}; Fig. 3 B and Tables S5 and S6). Notably, the highly significant changes in expression of genes involved in cell cycle and cell death pathways might account for the defects in meiotic divisions and the increased apoptosis observed in *Sam68*$^{-/-}$ testes. The microarray data were confirmed on 11 mRNA targets by real-time PCR (Fig. 3 C). The chosen targets included one up-regulated transcript, Riken 4931428L18, and 10 down-regulated transcripts. Among these, we chose those encoding for NEDD1, a centrosomal protein that is required for microtubule organization (Haren et al., 2006); SPDYA, a cell cycle regulator involved in oocyte meiotic maturation (Gastwirt et al., 2007); and SPAG16, a component of the sperm axoneme whose deficiency causes reduced spermatozoa motility and male infertility (Zhang et al., 2006). Actually, a deficiency in SPAG16 could be sufficient to contribute to the *Sam68*$^{-/-}$ infertility phenotype. The haploid marker *Prm2*, encoding for protamine 2, was unaffected in the *Sam68*$^{-/-}$ knockout testis.

To test the possibility that Sam68 is associated with polyadenylated mRNAs in pachytene spermatocytes, we performed an RNP capture assay with oligo (dT)–cellulose to capture polyA mRNAs and associated proteins (Grivna, et al., 2006). Under these conditions, Sam68 was efficiently retained by the oligo (dT)–cellulose, and this interaction was strongly impaired when spermatocyte cell extracts were treated with RNase A (Fig. 4 A), or when oligo (dT)–cellulose was preincubated with excess polyA but not polyC (Fig. 4 C). A similar result was obtained for the polyA-binding protein PABP1, which was used as the positive control of the experiment. These results indicate that Sam68 specifically interacts with polyadenylated RNA in mouse spermatocytes. Next, we asked whether the affected mRNAs are direct targets of Sam68 by coimmunoprecipitation experiments. In line with this hypothesis, we observed that all the mRNA targets tested specifically associated with Sam68 in RNP-immunoprecipitation experiments (Fig. 4 D). In contrast, *Muc3* and *Gapdh* mRNAs, which were not affected by Sam68 ablation, were not associated with the protein. Sam68 was immunoprecipitated by the specific antibody but not by control IgGs (Fig. 4 E). These results suggest that Sam68 directly regulates the expression of its mRNA targets in germ cells.

Sam68 associates with polyA mRNA engaged in translation

The major defects observed in *Sam68*$^{-/-}$ testes affected postmeiotic haploid cells. Interestingly, Sam68 localized in the cytoplasm in secondary spermatocytes (Figs. 5 A and S1) and some round spermatids (Fig. 5 B), which suggests a role in translational control. Translational regulation in eukaryotes is frequently exerted at the initiation step (Richter and Sonenberg, 2005), which normally depends on the m7GpppN 5′ cap structure of the mRNA. The mRNA 5′ cap recruits the 40S ribosome subunit via interaction with the cap-binding protein eIF4E and the scaffold protein eIF4G (Hay and Sonenberg, 2004; Richter and Sonenberg, 2005). These steps are assisted by additional RBPs, many of which are highly or uniquely expressed in germ cells (Venables and Eperon, 1999; Elliott, 2003; Kuersten and Goodwin, 2003; Lasko et al., 2005). To test whether Sam68 is able to interact with the translation initiation complex eIF4F, we incubated spermatocyte extracts with m7GTP-Sepharose beads. We found that Sam68 specifically bound the m7GTP-Sepharose in pachytene spermatocytes, and

is represented on the y axis. (C) Bar graph of the flow cytometry analyses from three independent experiments. Data are represented as mean ± SD. *, $P < 0.01$. (D) Electron microscopy of testicular sections from *Sam68*$^{-/-}$ mice. Images refer to different abnormalities that were frequently observed during spermiogenesis, such as abnormally divided spermatid nuclei (a), elongating spermatids with two flagella (b, arrows), binucleated elongated spermatids (c), and delayed spermatid differentiation, with step 9–10 spermatids (arrow) in stage XII tubules (d). Bars: (a) 0.4 µm; (b) 1 µm; (c) 0.7; (d) 2 µm. (E) Analysis of the number of spermatozoa found in the epididymis of *Sam68*$^{+/+}$ ($n = 7$), *Sam68*$^{+/-}$ ($n = 5$), and *Sam68*$^{-/-}$ ($n = 7$) mice. Approximately half of the 13 *Sam68*$^{-/-}$ mice ($n = 6$) analyzed had empty epididymis with no detectable spermatozoa and were not included in the experiment. Only the knockout mice that had residual spermatozoa were taken into account for this analysis. Data are represented as the mean ± SD. *, $P < 0.001$ in a *t* test and an ANOVA test.

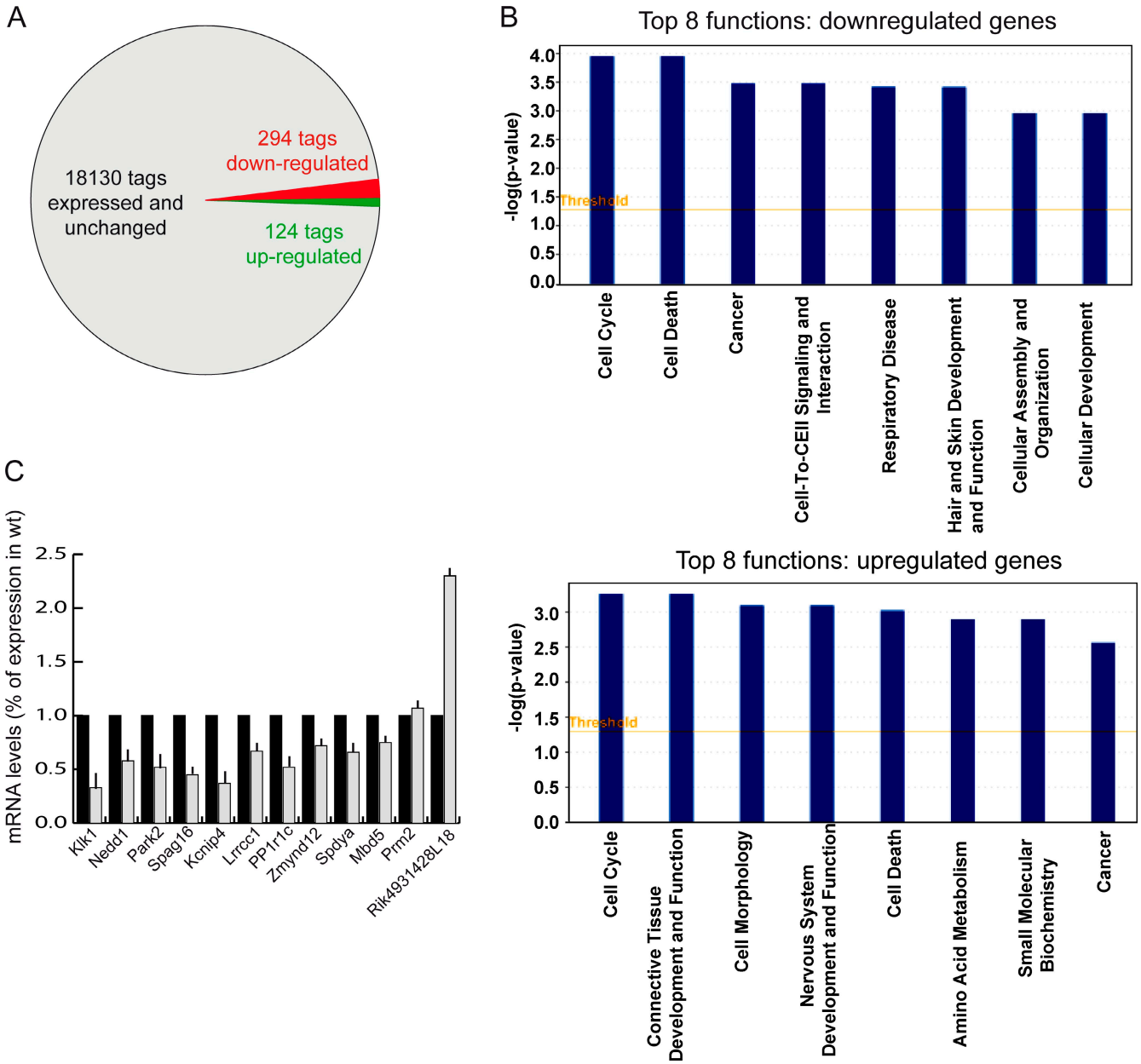

Figure 3. **Ablation of Sam68 affects expression of specific mRNAs in mouse testis.** (A) Diagram representing the differences in the transcriptome profile of mouse *Sam68*$^{+/+}$ and *Sam68*$^{-/-}$ testes. Three RNA preparations from different animals were used for each sample and independently hybridized on Affymetrix chips. Only tags whose differences gave a $P < 0.05$ in the *t* test analysis were reported. Unchanged expressed tags are represented in gray, down-regulated tags in red, and up-regulated tags in green. (B) The top eight functional categories that were significantly enriched among the genes down-regulated (top) or up-regulated (bottom) in the *Sam68* knockout testis. Analysis was performed using the IPA Ingenuity Systems. The range displayed corresponds to the most significant functions within high-level functional category. (C) Real-time PCR analysis of 10 of the mRNAs down-regulated in *Sam68*$^{-/-}$ testis. Data are represented as the mean ± SD of three separate experiments performed in duplicate.

that this interaction was strongly increased in extracts enriched in secondary spermatocytes (Fig. 5 C). Equal amounts of the mRNA 5′ cap-binding protein eIF4E and of eIF4G were pulled down in the two cell extracts. Remarkably, in somatic HEK293 cells, in which Sam68 is exclusively nuclear (Paronetto et al., 2007), no association with the eIF4F complex was observed (Fig. 5 D). These results demonstrate that Sam68 interacts with the translation initiation complex in male germ cells.

Sam68 associates with polysomes in secondary spermatocytes, and this cosedimentation in the "heavy" fractions required polysome integrity, as it was disrupted in the presence of EDTA (Fig. 5 E). A similar redistribution toward the RNP fractions was observed for PABP1 (Fig. 5 E), which is known to remain associated to mRNAs during translation (Collier et al., 2005). Thus, we next asked whether Sam68 was also bound to mRNAs engaged in translation on the polysomes. RNP-capture assays using the polysomal pool (1–5) of the fractionation of secondary spermatocyte-enriched extracts showed that polysome-associated Sam68 was captured by the oligo (dT)–cellulose, and that this interaction was counteracted by excess synthetic polyA RNA in the same manner as with PABP1 (Fig. 5 F). In line with the association of Sam68 with polyadenylated mRNA complexes in

germ cells, we found that Sam68 specifically associated with PABP1 in coimmunoprecipitation experiments using spermatocyte cell extracts (Fig. 5 G). These experiments suggest that Sam68 remains associated with polyadenylated mRNAs engaged in translation in male germ cells.

Sam68 is required for translation of *Spag16*, *Nedd1*, and *Spdya* mRNAs

To investigate whether Sam68 is required for polysomal recruitment of target mRNAs, we performed polysomal gradients using the germ cell population enriched in secondary spermatocytes and early round spermatids. RNA was purified from each of the 10 fractions of the gradients, and semiquantitative RT-PCR analyses were performed to determine the distribution of Sam68 target mRNAs (Fig. 6 A). Ablation of Sam68 did not affect the profile of polysomal gradients (unpublished data), demonstrating that it did not impair overall translation. Nevertheless, we observed that polysomal recruitment of *Spag16*, *Nedd1*, and *Spdya* mRNAs was decreased (Fig. 6 A). The distribution of these mRNAs in *Sam68*$^{+/-}$ cells formed two peaks, a larger peak in the RNP fractions and a smaller peak in the translationally active polysomal fractions (Fig. 6 A). Remarkably, only the polysomal peak was reduced in *Sam68*$^{-/-}$ cells. In contrast, *Gapdh* mRNA was equally distributed in sucrose gradients from *Sam68*$^{+/-}$ and *Sam68*$^{-/-}$ cells. This specific decrease in polysomal recruitment of *Spag16*, *Nedd1*, and *Spdya* mRNAs in *Sam68*$^{-/-}$ cells was confirmed by real-time PCR on polysomal and RNP fractions (Fig. 6 B). However, polysomal recruitment of the haploid cell–specific mRNAs *Tpn2* and *Prm2* was not impaired (Fig. 6 B), which indicates that the effects observed were not caused by alterations in the germ cell population. Consistent with the mRNA results, we found that SPAG16, NEDD1, and SPDYA proteins were strongly also reduced at the protein level in germ cells purified from *Sam68*$^{-/-}$ testes (Fig. 6, C and D). These results show that Sam68 is required for translation of specific target mRNAs during male germ cell differentiation.

Accumulation of SPAG16 and SPDYA proteins during the meiotic divisions requires Sam68

To determine whether the cytoplasmic translocation of Sam68 during the meiotic divisions of mouse spermatocytes favored translation of target mRNAs, we treated primary spermatocytes in culture with okadaic acid (OA). This serine/threonine phosphatase inhibitor triggers entry of pachytene spermatocytes into meiotic divisions (Wiltshire et al., 1995; Sette et al., 1999), which was visualized by staining with anti-phosphoH3 (Fig. S4 A). Interestingly, Sam68 translocated to the cytoplasm and associated with polysomes after brief treatment with OA (Fig. S4, B and C), and this coincided with its phosphorylation (Fig. 7 C), which is mediated by ERK1/2 (Paronetto et al., 2006). Moreover, we found that OA treatment stimulated the association of Sam68 with the eIF4F complex (Fig. 7 A). The effect was specific because association of eIF4G with eIF4E was instead decreased by OA treatment, probably due to induction of G2–M progression of primary spermatocytes and the general decrease in cap-dependent translation in cells approaching the metaphase

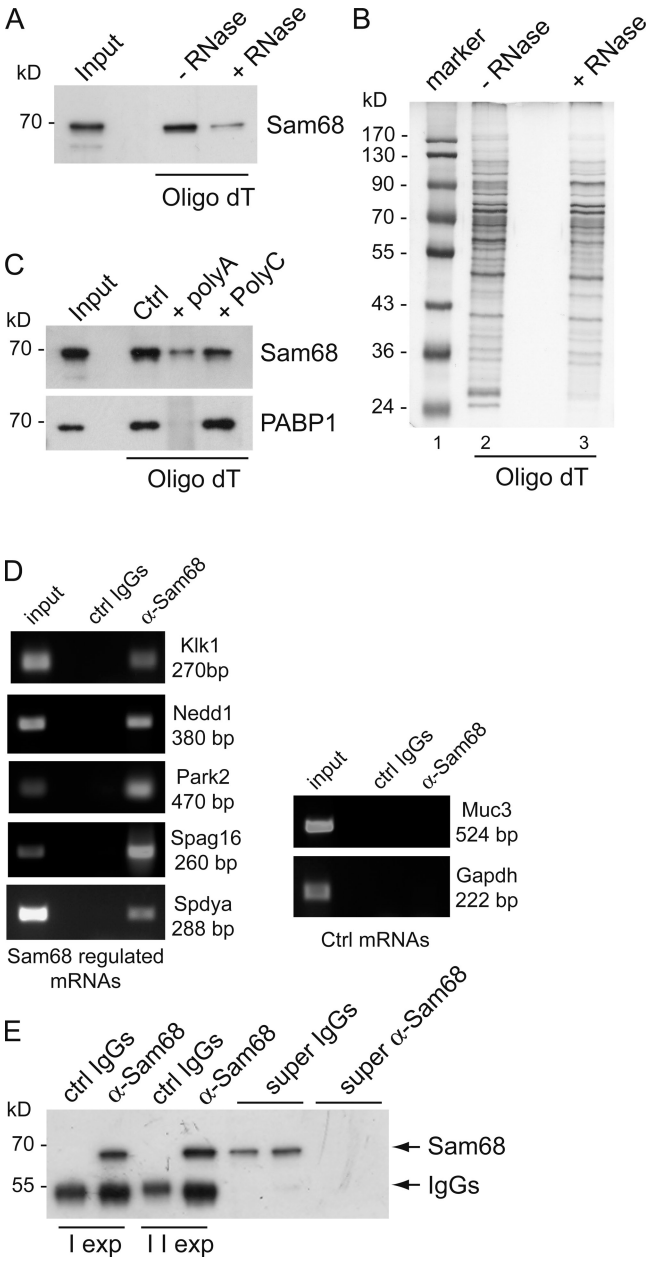

Figure 4. **Sam68 associates with selected polyadenylated mRNAs in mouse spermatocytes.** (A) RNP capture assay using oligo (dT)–cellulose beads and pachytene spermatocyte extracts in the presence or absence of RNase A. Proteins bound to the beads were analyzed by Western blotting with the anti-Sam68 antibody. (B) The same samples were separated by SDS-PAGE and detected by Silver staining. Molecular weight markers were loaded in the first lane. Silver staining of the gel shows that, although the pattern of bands changes, several proteins were bound to the oligo (dT) beads either in the absence or presence of RNase treatment, and that overall degradation of the sample did not occur under these conditions. (C) RNP capture assay of pachytene spermatocyte extracts were performed using oligo (dT)–cellulose beads left untreated (Ctrl) or pre-absorbed for 15 min with excess synthetic polyA or polyC RNA. Proteins bound to the beads were analyzed by Western blotting with the anti-Sam68 and the anti-PABP1 antibodies. (D) RT-PCR analysis of the enrichment in target mRNAs after co-immunoprecipitation with Sam68 from isolated wild-type germ cells. Two mRNAs that resulted in unchanged *Sam68*$^{-/-}$ testis, *Gapdh* and *Muc3*, were used as negative controls in the same experiment. (E) Western blot analysis of the quality of the control and anti-Sam68 (α-Sam68) immunoprecipitation experiments used for the RT-PCR analysis illustrated in D.

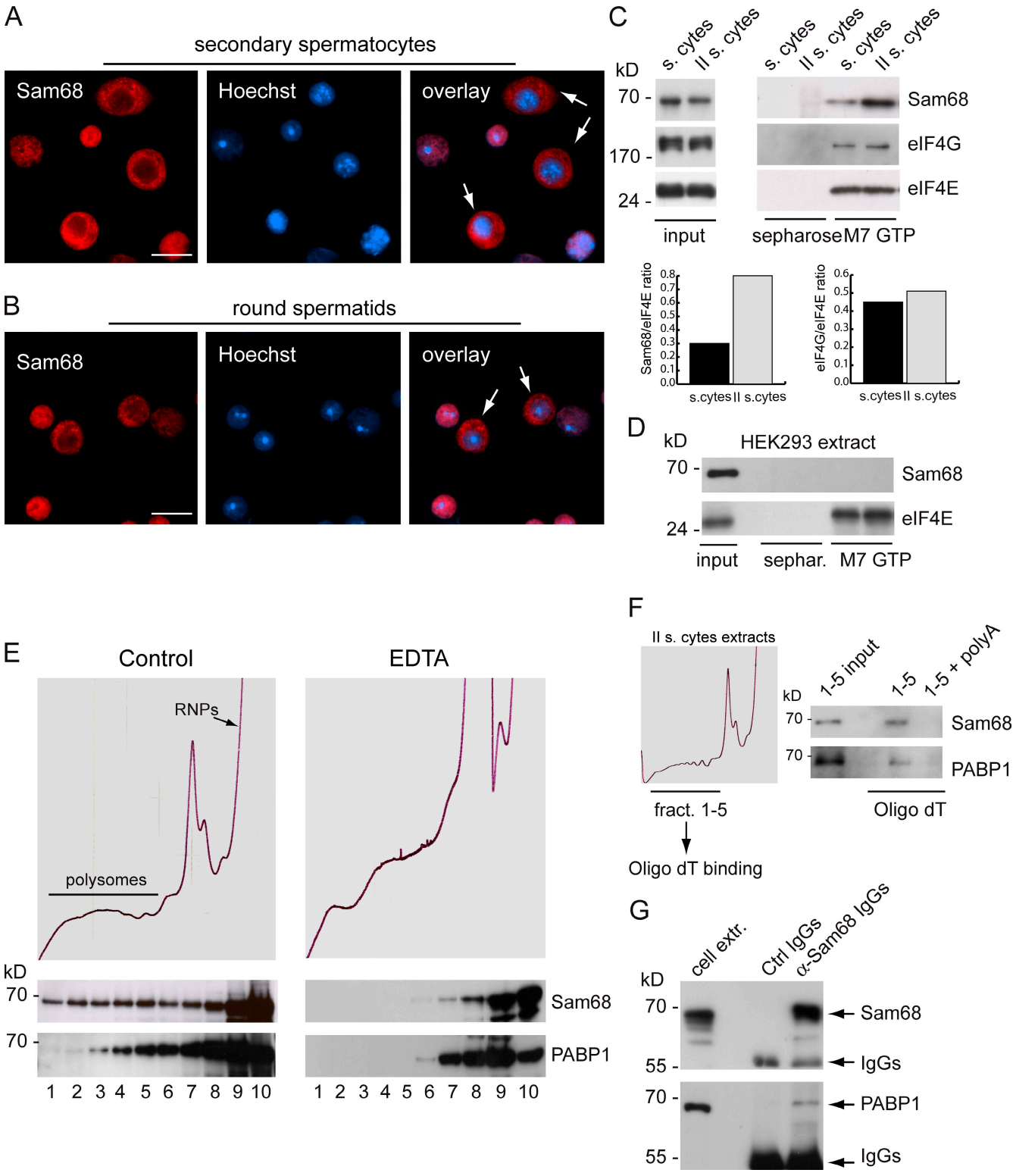

Figure 5. **Cytoplasmic Sam68 associates with polyadenylated mRNAs and the translational machinery in germ cells.** (A and B) Immunofluorescence analysis of germ cell populations enriched in secondary spermatocytes (A) or round spermatids (B) demonstrates that Sam68 is frequently localized in the cytoplasm in these cells. Representative examples of cytoplasmic localization are indicated by arrows. Bars, 10 µm. (C and D) Pull-down assay using the 5′-cap analogue m7GTP-Sepharose beads (M7GTP) to isolate the translation initiation complex from male germ cells (C) or HEK293 cells (D). Control pull-down assays were performed using Sepharose beads (sepharose). The panels show Western blot analysis of the Sam68, eIF4G, and eIF4E proteins in the input and bound in the pull-down assays using pachytene spermatocyte (s.cytes) extracts or extracts from a population enriched in secondary spermatocytes (II s.cytes) (C). Bottom panels show densitometric analysis of the pull-down assays. Data are represented as ratios between Sam68 and eIF4E or eIF4G and eIF4E band intensities. (E) Absorbance profile (OD = 254 nm) of sucrose gradient sedimentation of cell extracts from a population enriched in secondary spermatocytes. Extracts were either untreated (control) or treated with EDTA. The gradients were collected in 10 fractions, starting from the bottom heavy fractions, and the bottom panels show the Western blot analysis of Sam68 and PABP1 distribution in each fraction of the gradient. (F) RNP capture assay

(Pyronnet et al., 2001). To test whether this increased association with the eIF4F complex stimulated the translation of Sam68-targeted mRNAs, we analyzed SPAG16 and SPDYA protein levels, whose expression was increased in postmeiotic germ cells (Fig. 7 B). OA treatment of spermatocytes induced a time-dependent accumulation of SPAG16 and SPDYA proteins in *Sam68*$^{+/+}$ primary spermatocytes (Fig. 7 C) concomitantly with increased phosphorylation of Sam68, as indicated by the shift in molecular weight (Matter et al., 2002; Paronetto et al., 2006), and with its association with polysomes (Fig. S4 C). Densitometric analysis using tubulin as an internal standard showed that SPAG16 levels almost doubled and SPDYA sharply accumulated by 6 h of treatment (Fig. 7 C). Remarkably, this accumulation was almost completely suppressed in knockout spermatocytes, demonstrating that translation of these proteins during the meiotic divisions requires Sam68. The increases in protein levels were not caused by enhanced stabilization or cytoplasmic export of the mRNAs, because similar levels of *Spag16* and *Spdya* transcripts were detected in cytoplasmic extracts during the time course of the experiment (Fig. 7 D).

To determine whether Sam68 directly enhanced translation of a target transcript, we transfected HEK293 cells with Sam68 and a luciferase reporter construct with or without the *Spag16* 3′ untranslated region (UTR; Fig. 8 B). Although Sam68 was exclusively localized in the nuclei of HEK293 cells, coexpression of a constitutively active form of RAS (RASL61Q) induced its cytoplasmic translocation and association with polysomes (Fig. 8 A), which correlated with activation of ERK1/2, as in germ cells (Paronetto et al., 2006). Under these conditions, Sam68 strongly enhanced expression of luciferase only in the presence of *Spag16* 3′ UTR. Moreover, the effect relied on extracellular signal-regulated kinase (ERK)-dependent phosphorylation, because a Sam68 mutant in which the phosphorylation sites were substituted (Matter et al., 2002) was unable to induce luciferase expression (Fig. 8 B). To determine whether the increased expression was caused by enhanced polysomal loading of the reporter mRNA, we isolated polysomal- and RNP-associated mRNAs from these samples. As shown in Fig. 8 C, although the total cytoplasmic levels of luciferase mRNA were similar, expression of wild-type Sam68 increased polysomal recruitment of the reporter mRNA, whereas the phosphorylation mutant was inefficient. These data indicate that phosphorylation of Sam68 by ERKs stimulates translation of target mRNAs.

Discussion

Posttranscriptional regulation of gene expression is essential for the progression of spermatogenesis. A large number of mRNAs need to be accumulated during the transcriptionally active stages of germ cell differentiation and translated later on to account for the lack of transcription that occurs during homologous recombination and sperm differentiation (Kleene, 2001). RBPs are highly expressed in germ cells and likely account for this posttranscriptional regulation. The results presented herein demonstrate that the RBP Sam68 is absolutely required for male fertility and for the correct progression of spermatogenesis. The defects in germ cell differentiation were accompanied by increased apoptosis and a large reduction in haploid spermatids, which failed to differentiate into correctly shaped and fully motile spermatozoa.

The defective spermatogenesis observed in *Sam68*$^{-/-}$ mice is unlikely to be caused by androgen imbalance, as testosterone levels in the serum were normal, and a comparison of the mRNAs altered in *Sam68*$^{-/-}$ testis with those affected by deletion of the androgen receptor (Gene Expression Omnibus profiles found at http://www.ncbi.nlm.nih.gov) revealed no overlap (unpublished data). Our microarray analyses identified the first mRNAs affected by Sam68 ablation in a physiological setting. The changes in mRNA expression were not caused by the altered germ cell population (i.e., a decrease in haploid cells) because transcripts for well-defined markers of postmeiotic differentiation, such as those encoding protamine 2 and transition protein 2, were not altered in *Sam68*$^{-/-}$ testis. Remarkably, the top represented categories among the mRNA down-regulated in *Sam68*$^{-/-}$ testis were cell cycle and cell death. Because the first obvious defect in spermatogenesis appears at the time when the meiotic divisions occur and correlate with increased apoptosis, our analyses suggest that these phenotypes might be due to the lower levels of expression of several genes involved in these processes. We also found an enrichment of genes involved in cancer, in line with the recently discovered role of Sam68 in prostate cancer (Busà et al., 2007), breast cancer (Richard et al., 2008), and mixed lineage leukaemia (*MLL*; Cheung et al., 2007). Thus, our microarray data provide a first list of genes potentially involved in the function of Sam68 in cancer cells. Moreover, the identification of mRNAs physiologically affected by Sam68 in testis might also provide valuable information for transcripts regulated by this RBP in other tissues in which its ablation caused a phenotype, such as bone and brain (Richard et al., 2005; Lukong et al., 2008; Chawla et al., 2009).

Although we have investigated the regulation of mRNAs down-regulated in the Sam68 knockout testis, other transcripts were up-regulated. The mechanism leading to these increased levels is likely different from the translational regulation of selected targets described herein. Sam68 is nuclear in premeiotic germ cells, and it is possible that nuclear events are causing the observed up-regulation. For instance, Sam68 might stabilize target transcripts during their storage in the nucleus of meiotic cells. Alternatively, because Sam68 was found to repress viral and cellular promoters in somatic cells (Lukong and Richard, 2003), it is possible that some of the observed up-regulations are caused by the relief of such transcriptional inhibitory function of the protein.

Our results suggest that Sam68 is implicated in the regulation of translation of its target mRNAs in germ cells. First, we observed that Sam68 associates with mRNAs that are

using oligo (dT)–cellulose beads in the presence or absence of excess free polyA synthetic RNA and polysomal (1–5) fractions derived from sucrose gradient fractionation of cell extracts as described in E. The input loaded in the pull-down experiment and the proteins bound to the beads were separated by SDS-PAGE and immunoblotted with the anti-Sam68 antibody. (G) Western blot analysis of the coimmunoprecipitation between Sam68 and PABP1 from germ cell extracts. Samples were immunoprecipitated with either nonimmune (Ctrl) or anti-Sam68 (α-Sam68) IgGs. Immunoprecipitated proteins were separated on 10% SDS-PAGE and immunoblotted with anti-Sam68 or anti-PABP1 antibodies.

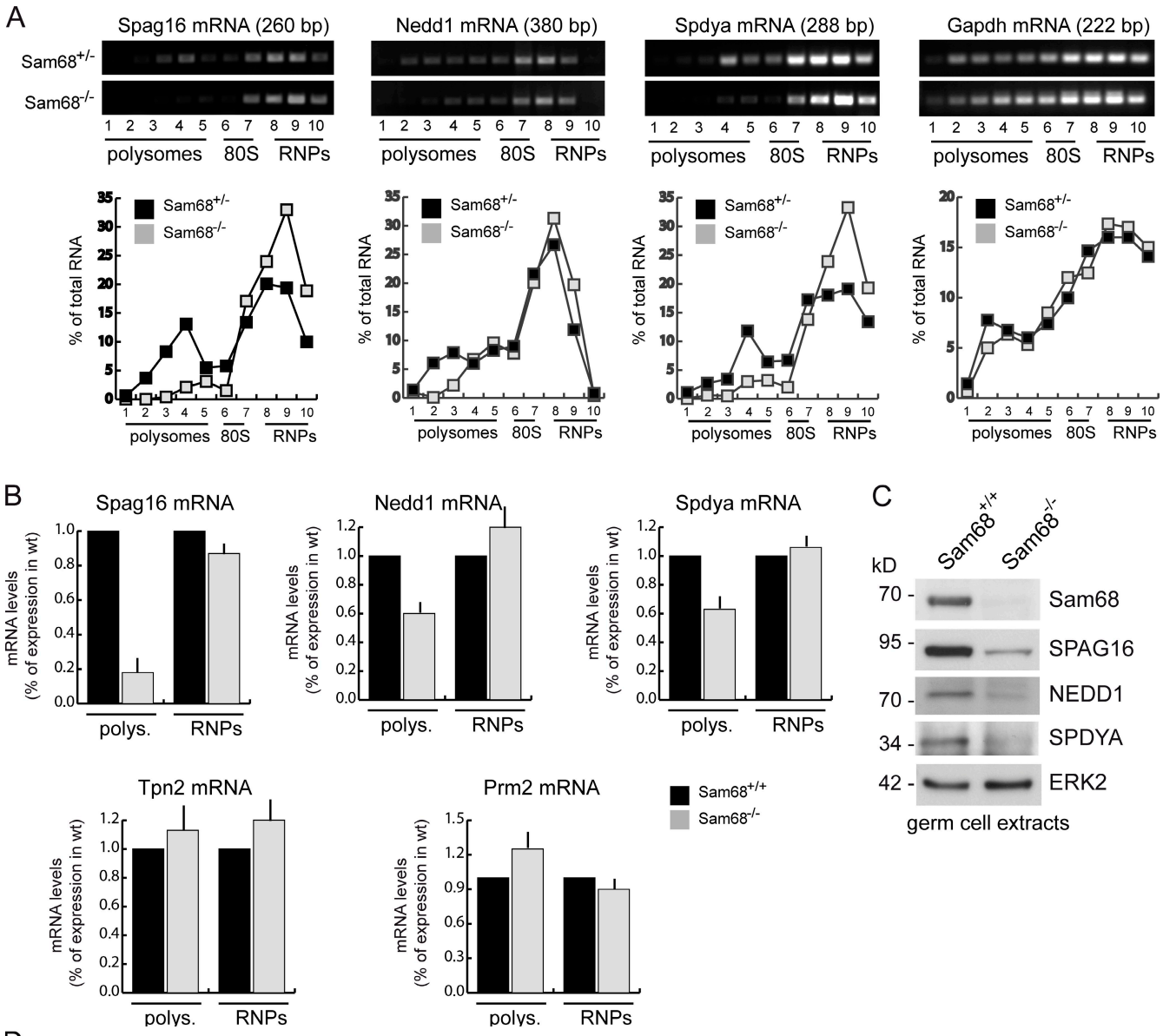

Figure 6. **Sam68 enhances translation of *Spag16*, *Nedd1*, and *Spdya* mRNAs in germ cells.** (A) RT-PCR analysis of the distribution of *Spag16*, *Nedd1*, *Spdya*, or *Gapdh* mRNAs in the fractions of the sucrose gradients derived from sucrose gradient fractionation of germ cell extracts from *Sam68*$^{+/-}$ or *Sam68*$^{-/-}$ mice. Densitometric analysis of the signal in each fraction was performed, and the results were represented as the percentage of total signal in all fractions in the bottom panels. (B) Quantitative real-time PCR analysis of *Spag16*, *Nedd1*, *Spdya*, *Tpn2*, and *Prm2* mRNA levels in the polysomal (1–5) and RNP (8–10) fractions. *Gapdh* mRNA was used as an internal standard for the real-time PCR analysis. (C) Western blot analysis of Sam68, SPAG16, NEDD1, and SPDYA proteins in germ cells isolated from *Sam68*$^{+/+}$ or *Sam68*$^{-/-}$ testes. ERK2 was used as a loading control. (D) Immunofluorescence analysis of SPAG16 and NEDD1 proteins in germ cells isolated from *Sam68*$^{+/+}$ or *Sam68*$^{-/-}$ testes. Hoechst costaining was performed to distinguish pachytene spermatocytes (Pc) from round spermatids (Spt). Bars, 10 µm.

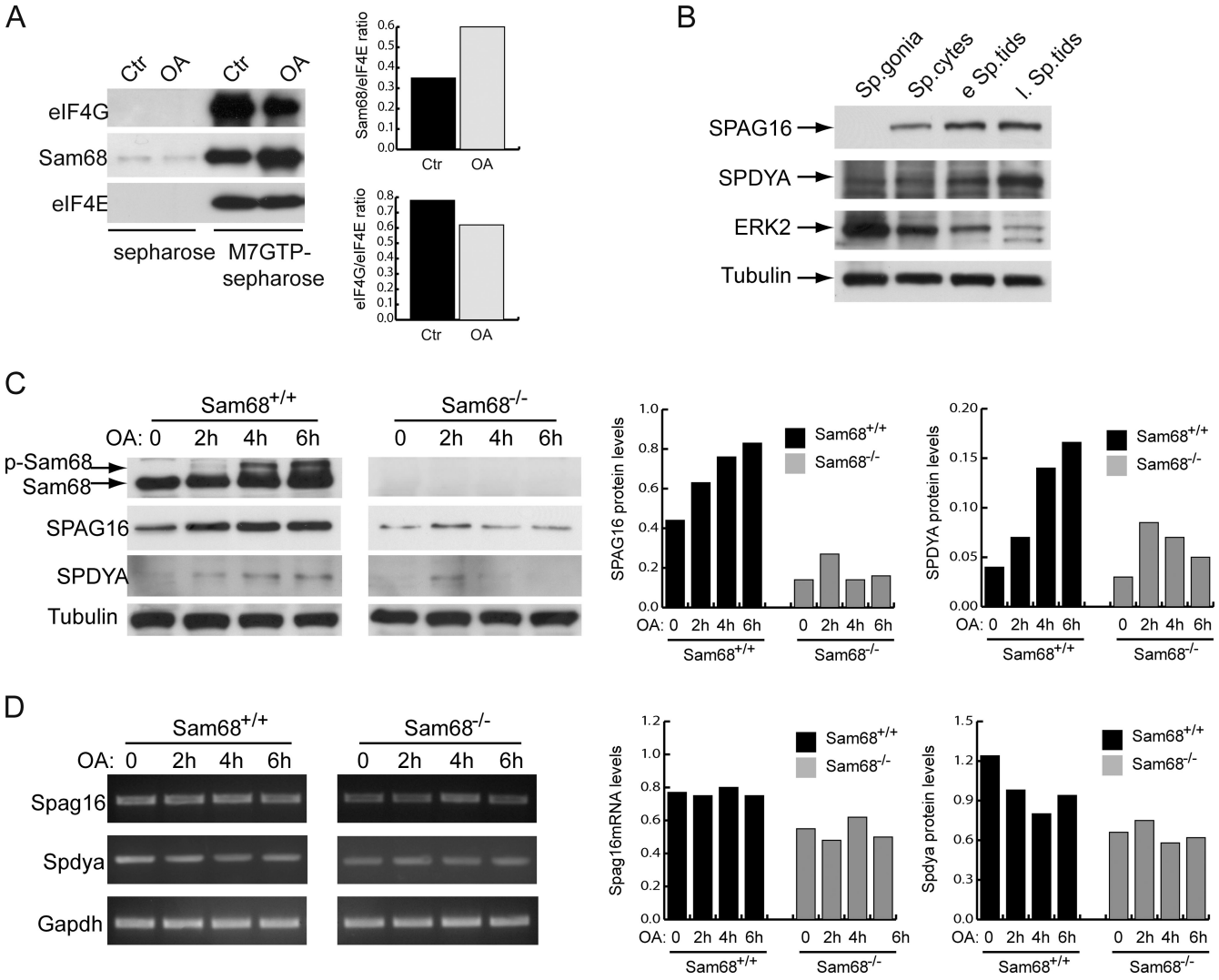

Figure 7. **Sam68 is required for *Spag16* and *Spdya* mRNA translation during the meiotic divisions.** (A) m7GTP-Sepharose bead (M7GTP-sepharose) pull-down assays using extracts from pachytene spermatocytes (Ctrl) or spermatocytes treated with 0.5 µM OA (OA). Control pull-down assays were performed using Sepharose beads (sepharose). Western blot analysis of the Sam68, eIF4G, and eIF4E proteins bound in the pull-down assays are shown as indicated. Bottom panels show the densitometric analysis of the pull-down assays. Data are represented as ratios between Sam68 and eIF4E or eIF4G and eIF4E band intensities. (B) Western blot analysis of the expression levels of SPAG16 and SPDYA proteins in germ cells at different stages of differentiation. ERK2 and tubulin staining were also performed as a control of loading to rule out a general increase in proteins. (C and D) Western blot (C) or RT-PCR (D) analyses of extracts from *Sam68*$^{+/+}$ or *Sam68*$^{-/-}$ pachytene spermatocytes before (0) or after treatment with 0.5 µM OA for 2, 4, or 6 h. (C) The top panel shows the levels of Sam68 and its shift in electrophoretic mobility caused by phosphorylation (p-Sam68) after OA treatment. The middle panels show the accumulation of SPAG16 and SPDYA in *Sam68*$^{+/+}$ spermatocytes, and the bottom panel shows tubulin as loading control of the experiment. The bar graphs show the densitometry of SPAG16 and SPDYA protein expression expressed as a ratio with the intensity of tubulin in each lane analyzed. (D) The bar graphs show the densitometry of *Spag16* and *Spdya* mRNA levels expressed as a ratio with the intensity of *Gapdh* in each lane analyzed.

down-regulated in the knockout testis, which suggests that these represent its mRNA targets in germ cells. Moreover, we provide strong evidence that Sam68 interacts with the translational machinery in germ cells and favors translation of specific mRNAs. Sam68 binds to the translation initiation complex eIF4F and remains associated with polyadenylated mRNAs in the polysomal fraction, which strongly suggests its stable interaction with mRNAs engaged in translation. In line with this hypothesis, we demonstrate that Sam68 is required for efficient polysomal loading of three target mRNAs (*Spdya*, *Nedd1*, and *Spag16*) and that the corresponding proteins are not accumulated in *Sam68*$^{-/-}$ germ cells undergoing meiotic divisions or early spermatid differentiation. The effect on translation appears direct because it can be recapitulated in a heterologous system by adding the 3′ UTR region of a Sam68 target mRNA to the luciferase reporter gene. Remarkably, Sam68 function requires ERK-dependent phosphorylation both for the association with polysomes and the enhancement of luciferase mRNA translation, similar to what was observed in meiotic germ cells. Thus, our results highlight a novel role of Sam68 in translational regulation and indicate that the binding of Sam68 to its target mRNAs in the cytoplasm favors their translation during the meiotic progression of mouse spermatocytes (Fig. 9). Remarkably, SPAG16 deficiency leads to defects in sperm motility and male infertility (Zhang et al., 2006), which closely resembles the phenotype of Sam68 knockout mice. These observations suggest that the strong reduction in

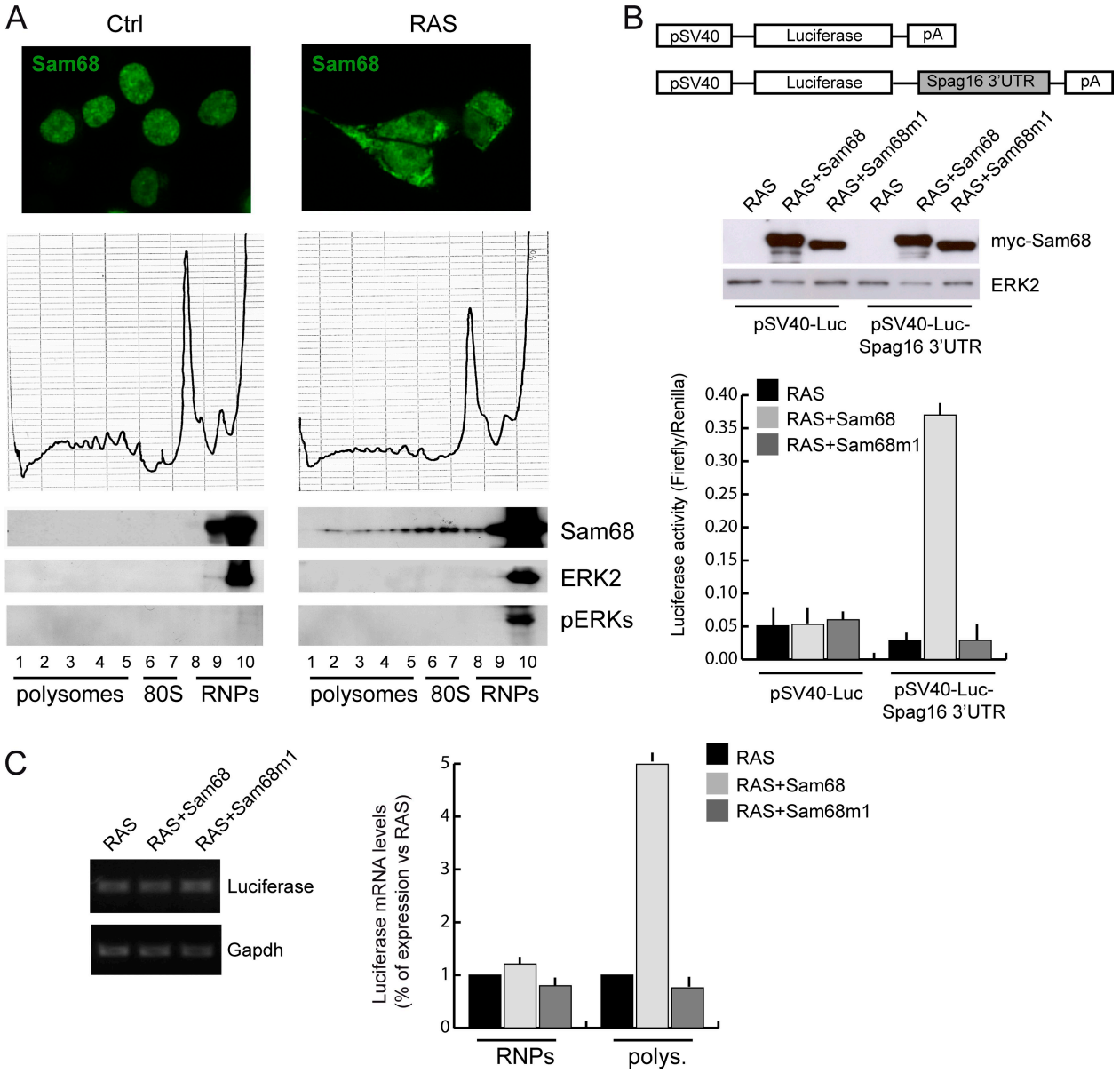

Figure 8. **Sam68 enhances translation of a reporter gene containing the 3′ UTR of the *Spag16* mRNA.** (A) HEK293 cells were transfected with a construct expressing GFP-Sam68 in the absence (left) or presence (right) of a construct encoding a constitutively active form of RAS (RASL61Q), which induces cytoplasmic translocation of the protein. The absorbance profile (OD = 254 nm) of sucrose gradient sedimentation of cells extracts from control (Ctrl) or RAS-transfected (RAS) cells are shown. The bottom panels show the Western blot analysis of Sam68 distribution in each fraction of the gradients. Fractions were also analyzed for ERK2 and for phosphoERKs (pERKs) to determine the activation of mitogen-activated kinases downstream of RAS. (B) Luciferase reporter assay of the effect of wild-type or mutated Sam68 (Sam68m1) on the expression of luciferase in the presence or absence of the 3′ UTR of Spag16 mRNA. HEK293 cells were cotransfected with empty vector, mycSam68, or mycSam68m1 and a constitutively active form of RAS to induce cytoplasmic translocation and polysome association of Sam68. A schematic representation of the Firefly luciferase constructs used is shown above the graph. Western blot analysis of the expression of wild-type and mutant mycSam68 is shown. Western blotting for ERK2 was performed as a loading control. The data of the reporter assay are expressed as the mean ± SD of three experiments and represented as ratios between Firefly and Renilla luciferase activity in each sample. (C) Extracts from HEK293 cells transfected with the Luciferase-Spag16 reporter gene and RAS alone or in combination with wild-type or mutant Sam68 were separated on sucrose gradients, then RNA was isolated from each fraction and pools of the polysomal (1–5) or RNP (8–10) fractions were used for real-time PCR as described in Fig. 6 B using *Gapdh* as the internal standard.

SPAG16 translation observed in *Sam68*$^{-/-}$ germ cells contributes to the infertility of the knockout mice and provides functional support for the role of Sam68 in the cytoplasm of male germ cells. A role for Sam68 in mRNA translation might also be envisioned in biological contexts in which Sam68 translocates to the cytoplasm, such as in the course of viral infections (McBride et al., 1996), when it favors cytoplasmic utilization of viral mRNAs (Coyle et al., 2003), or in response to depolarization of neurons (Ben Fredj et al., 2004).

The role of Sam68 in RNA biogenesis has been recently unraveled. This RBP can strongly modulate the choice of alternative exons for the *CD44*, *Sgce*, and *BCL-x* pre-mRNA (Matter et al., 2002; Cheng and Sharp, 2006; Paronetto et al., 2007; Chawla et al., 2009). Alternative splicing is tightly connected to transcription

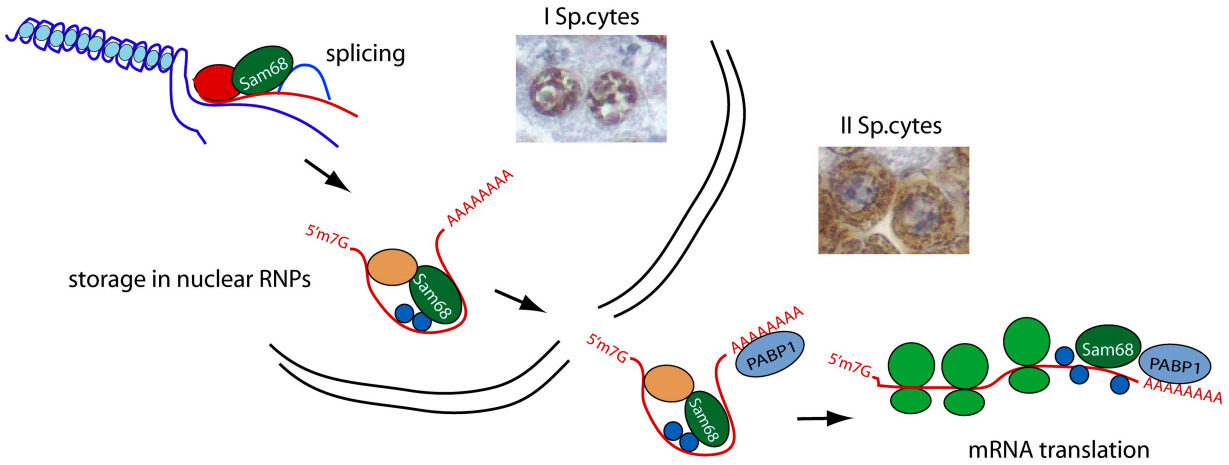

Figure 9. **Schematic model of the role of Sam68 in male germ cells.** Upon meiotic divisions, Sam68 is released in the cytoplasm and enhances translation of mRNAs bound to it, such as those encoding for SPAG16 and SPDYA proteins. Insets show the localization of Sam68 detected by immunohistochemistry in primary and secondary spermatocytes.

(Kornblihtt et al., 2004; Bentley, 2005), and Sam68 was found to associate with the transcriptional regulatory complex SWI–SNF and to influence the choice of exons on nascent pre-mRNAs (Batsché et al., 2006). Although we studied the cytoplasmic role of Sam68, we observed that this RBP is nuclear in primary spermatocytes and in round spermatids from stage III through stage VIII (Fig. S1). Thus, it is possible that Sam68 regulates alternative splicing in these stages of germ cell differentiation. The dual role of Sam68 in alternative splicing and translational regulation is not unique to this RBP. Other splicing regulators have been recently described to play a role in mRNA translation. For instance, hnRNP A1 translocates to the cytoplasm after several types of cellular stress, and can favor or inhibit translation of specific target mRNAs (Cammas et al., 2007). In addition, the SR protein ASF/SF2 shuttles between the nucleus and cytoplasm in somatic cells, in a phosphorylation-dependent manner like Sam68, and associates with polysomes (Sanford, et al., 2005). More recently, it has been shown that ASF/SF2 associates with the eIF4F complex, as well as with mammalian target of rapamycin (mTOR) and the phosphatase PP2A, and that it regulates translation initiation through modulation of phosphorylation of the eIF4E-binding protein 4E-BP1 (Michlewski, et al., 2008). Sam68 belongs to a family of RBPs known to link signal transduction with RNA metabolism (Volk et al., 2008). Thus, because polysomal association of Sam68 correlates with its phosphorylation during the meiotic divisions, our results suggest a new mechanism for Sam68-mediated translational regulation of specific mRNAs during cell cycle transitions.

In conclusion, our findings identify a novel function of Sam68 in male fertility and suggest that its loss of function results in defective protein translation of selected mRNAs and might represent the cause of certain cases of human male infertility.

Materials and methods

Analyses of *Sam68*$^{-/-}$ mice

The *Sam68* colony was maintained by intercrossing *Sam68*$^{+/-}$ mice. Genotyping of the mice was performed as described previously (Richard et al., 2005). For hematoxylin and eosin staining, testes were fixed in bouin's solution for 2 h, embedded in paraffin, and sectioned using standard protocols. For TUNEL analyses, testes were fixed in 4% paraformaldehyde in PBS for 12 h at 4°C. Immunohistochemical staining was performed on 5-µm-thick sections using the In Situ Cell Death Detection kit (Roche) according to manufacturer's instructions. For transmission electron microscopy, samples were fixed in 2.5% glutaraldehyde in 0.1 M cacodylate buffer, postfixed in 1% OsO_4, then dehydrated in ethanol and embedded in epon. Semithin sections were stained in toluidine blue, and thin sections were conventionally contrasted with uranyl acetate and lead hydroxide. Thin sections were examined and photographed in an electron microscope (Hitachi 7000; Hitachi).

Analyses of the fertility of *Sam68*$^{-/-}$ male mice

Sam68$^{+/-}$ (n = 5) and *Sam68*$^{-/-}$ (n = 6) mice were bred for 5 mo with wild-type females of proven fertility. Females were changed each time they remained pregnant or after 2.5 mo without remaining pregnant. To obtain fertilized oocytes, 6–7-wk-old B6D2F1 female mice (Charles River Laboratories) were hormonally primed by injecting 5 IU of pregnant mare's serum gonadotropin (PMSG; Intervet), and, after 46–48 h, 5 IU human chorionic gonadotropin (hCG; Intervet). Then *Sam68*$^{+/+}$, *Sam68*$^{+/-}$, or *Sam68*$^{-/-}$ males were added to the cage. Mating was scored 16 h later by monitoring the vaginal plugs. Oocytes and embryos were collected in freshly prepared M2 medium (Hogan et al., 1994) and scored for the presence of pronuclei as described previously (Sette et al., 2002). In vitro fertilization was performed using oocytes collected from hormonally primed B6D2F1 female mice and spermatozoa collected from *Sam68*$^{+/+}$, *Sam68*$^{+/-}$, or *Sam68*$^{-/-}$ males as described previously (Hogan et al., 1994). Statistical analyses were performed using the *t* test and the analysis of variance (ANOVA) test in all the experiments.

Cell isolation, culture, and treatments

Testes from 20–60-d-old CD1 mice (Charles River Laboratories) were used to obtain pachytene spermatocytes, secondary spermatocytes, and round spermatids by elutriation technique as described previously (Sette et al., 1999; Paronetto et al., 2006). FACS analysis of DNA content was performed as described previously (Paronetto et al., 2006; Busà et al., 2007). For TUNEL analysis, cells were labelled using the In Situ Cell Death Detection kit according to manufacturer's instructions.

After elutriation, pachytene spermatocytes were cultured in minimum essential medium (Invitrogen) and supplemented with 0.5% BSA (Sigma-Aldrich), 1 mM sodium pyruvate, and 2 mM lactate at 32°C in a humidified atmosphere containing 95% air and 5% CO2. Cells were treated overnight with 10 µM U0126 (EMD) before the addition of DMSO (Sigma-Aldrich) or 0.5 µM OA (EMD). Cultures were continued for an additional 4–6 h to induce metaphase entry. At the end of the incubation, cells were collected, washed with PBS, and used for experiments. HEK293 were cultured in DME containing 10% fetal bovine serum and transfected using the Fugene reagent (Roche). Luciferase reporter assays were performed as described previously (Loiarro et al., 2007).

Immunoprecipitation experiments

Isolated mouse germ cells were washed with PBS and then homogenized in lysis buffer (100 mM NaCl, 10 mM $MgCl_2$, 30 mM Tris-HCl, pH 7.4, 1 mM DTT, and protease inhibitor cocktail [Sigma-Aldrich]) supplemented with 0.5% Triton X-100 (Sigma-Aldrich). For protein–RNA coimmunoprecipitation,

40 U/ml RNase OUT (Invitrogen) was added to the extracts. Soluble extracts were separated by centrifugation at 10,000 *g* for 10 min, and then precleared for 2 h on protein A–Sepharose beads (Sigma-Aldrich) in the presence of 5 µg of rabbit IgGs, 0.05% BSA, and 0.1 µg/ml yeast tRNA. After centrifugation for 1 min at 1,000 *g*, supernatants were incubated with 5 µg of anti-Sam68 (Santa Cruz Biotechnology, Inc.) or 5 µg of rabbit IgGs for 3 h at 4°C under constant rotation. After washing, an aliquot of the beads was eluted in SDS sample buffer for Western blot analysis. The remaining beads were incubated with lysis buffer in the presence of (RNase-free) DNase (Roche) for 15 min at 37°C, and washed three times with lysis buffer before incubation with 50 µg of proteinase K (Roche) for an additional 15 min at 37°C. Coprecipitated RNA was then extracted by standard procedure and used for RT-PCR or microarray analysis.

RT-PCR analysis

RNA polysomal fractions were used for RT-PCR using M-MLV reverse transcriptase (Invitrogen) according to manufacturer's instructions. 10% of the reverse-transcription reaction was used as template. Quantitative real-time PCR on total, RNP, and polysomal RNAs were performed in triplicate using iQ Sybr-green Supermix (Bio-Rad Laboratories) according to manufacturer's instructions, as described previously (Bianchini et al., 2008). *Gapdh* was used to obtain the ΔΔCt values for the calculation of fold increases.

Microarray analysis

Total testis RNA from adult $Sam68^{+/+}$ ($n = 3$) and $Sam68^{-/-}$ ($n = 3$) mice was extracted using TRIZOL reagent (Invitrogen), followed by clean up on RNeasy mini/midi columns (RNeasy Mini/Midi kit; QIAGEN). Adult mice were used to minimize differences in haploid cell population observed in juvenile animals. Approximately 2% of the genes expressed in testis were affected by Sam68 ablation. Biotin-labeled cRNA targets were synthesized starting from 5 µg of total RNA according to the Affymetrix protocol (Rossi et al., 2008). The size and the quality of RNA targets was checked by agarose gel electrophoresis before and after fragmentation. Targets were diluted in hybridization buffer and hybridized to GeneChipMOE430 version 2.0 arrays (Affymetrix) as described previously (Rossi et al., 2008). Data were analyzed through the use of IPA Ingenuity Systems (www.ingenuity.com). 400 out of the 418 known tags entered were mapped in specific network and functional categories. The p-value associated with functions or pathways in IPA is a measure of the likelihood that the association between a set of focus molecules in the experiment and a given function or pathway is due to random chance. A smaller p-value (<0.05) indicates that the association was significant rather than random. The p-value is calculated using the right-tailed Fisher's exact test.

Polysome–RNP fractionation by sucrose gradients

Isolated germ cells were homogenized in lysis buffer (100 mM NaCl, 10 mM $MgCl_2$, 30 mM Tris-HCl, 1 mM DTT, and protease inhibitor cocktail [Sigma-Aldrich]) and 40 U/ml RNase OUT (Invitrogen) supplemented with 0.5% Triton X-100. After 10 min of incubation on ice, the lysates were centrifuged for 10 min at 12,000 *g* at 4°C. The supernatants were separated on 15–50% (wt/vol) sucrose gradients, and proteins and RNA were collected in 10 fractions as described previously (Paronetto et al., 2006). For EDTA-treated samples, $MgCl_2$ in the buffers was replaced with 20 mM EDTA. The incubation was performed for 15 min at room temperature and stopped by adding 3 mM EGTA.

7-methyl-GTP-Sepharose pull-down assay

For the isolation of eIF4E and associated proteins, cells were lysed in buffer containing 50 mM Hepes, pH 7.4, 75 mM NaCl, 10 mM $MgCl_2$, 1 mM DTT, 8 mM EGTA, 10 mM β-glycerophosphate, 0.5 mM Na_3VO_4, 0.5% Triton X-100, and protease inhibitor cocktail. Cell extracts were incubated for 10 min on ice and centrifuged at 12,000 *g* for 10 min at 4°C. The supernatants were precleared for 1 h on Sepharose beads (Sigma-Aldrich). After centrifugation for 1 min at 1,000 *g*, supernatants were recovered and incubated for 2 h at 4°C with 7-methyl-GTP-Sepharose or control Sepharose (GE Healthcare) under constant shaking. Beads were washed three times with lysis buffer, and absorbed proteins were eluted in SDS-PAGE sample buffer.

Western blot analysis

Western blot analyses were performed as described previously (Sette et al., 2002). The following primary antibodies (1:1,000 dilution) were used: rabbit anti-Sam68 and rabbit anti-Erk2 (Santa Cruz Biotechnology, Inc.); rabbit anti-phosphoERKs, anti-eIF4E, and eIF4G (Cell Signaling Technology); rabbit anti-SPAG16 (provided by J.F. Strauss, Virginia Commonwealth University, Richmond, VA; Zhang et al., 2006), mouse anti-tubulin, and rabbit anti-actin (Sigma-Aldrich); rabbit anti-SPDYA (EMD); and rabbit anti-NEDD1 and rabbit anti-PABP1 (Abcam). Immunostained bands were detected by the chemiluminescent method (Santa Cruz Biotechnology, Inc.). Densitometric analysis was performed using the ImageQuant 5.0 software (GE Healthcare) and normalized for the tubulin or eIF4E staining.

Immunofluorescence analysis

Mouse germ cells were fixed in 4% paraformaldehyde and washed three times with PBS. Cells were permeabilized with 0.1% Triton X-100 for 7 min and then incubated for 1 h in 0.5% BSA. Cells were washed three times with PBS and incubated for 2 h at room temperature with antibodies against Sam68 (1:1,000), phosphor-H3 (1:1,000; Millipore), SPAG16 (1:200), or NEDD1 (1:200) followed by 1 h of incubation with cy3-conjugated anti–mouse IgGs (Alexa Fluor) or FITC-conjugated anti–rabbit IgGs (Alexa Fluor). After washes, slides were mounted with Mowiol reagent (EMD) and analyzed by microscopy using an inverted microscope (DMI6000B; Leica).

Image acquisition and manipulation

Images were taken from a fluorescent microscope (Axioskop; Carl Zeiss, Inc.) using a Pan-Neofluar 40×/0.75 objective lens, and from an inverted microscope (DMI6000B; Leica) using a Pan-Neofluar 40×/0.75 objective lens. Images were acquired at room temperature using an RT slider camera (Diagnostic Instruments) and the IAS2000 software (Biosistem 82) or LIF software (Leica). Images were acquired as TIFF files, and Photoshop and Illustrator software (Adobe) was used for composing the panels.

Online supplemental material

Fig. S1 shows stage-specific expression of Sam68 in mouse testis. Fig. S2 shows testis and body weight, testosterone levels, and apoptosis analysis in wild-type, heterozygote, and knockout Sam68 mice. Fig. S3 shows a developmental analysis of testicular morphology in Sam68 wild-type and knockout mice. Fig. S4 shows phosphoH3 and Sam68 immunofluorescence analysis in control and OA-treated spermatocytes, and sucrose gradient fractionation of extracts from the same cells. Tables S1–S6 show the results of the microarray and IPA analyses of mRNAs from wild-type and knockout testes. Videos S1–S3 show the motility phenotype of wild-type and knockout spermatozoa. Online supplemental material is available at http://www.jcb.org/cgi/content/full/jcb.200811138/DC1.

The authors wish to thank Dr. Jerome F. Strauss III for the generous gift of the anti-SPAG16 antibody, Dr. Harald Konig for the gift of the mycSam68m1 and RASL61Q plasmids, Dr. Maria Loiarro for assistance with luciferase reporter assays, Dr. Flavia Botti for assistance with histochemical analysis, Dr Simona Pedrotti for assistance with germ cell purification, and Amber Zabarauskas for assistance with IPA analyses. We wish to thank Dr Daniela Barilà and members of our laboratories for critical reading of the manuscript.

This work was supported by grants from Telethon (GGP01488 to C. Sette), the Associazione Italiana Ricerca sul Cancro (to C. Sette and M. Barchi), the Lance Armstrong Foundation (to C. Sette), the Istituto Superiore della Sanità (Project no. 527/B/3A/5 to C. Sette and R. Geremia), the Italian Ministry of Education (PRIN 2004 and 2005 to C. Sette and R. Geremia), and the Canadian Institutes of Health Research (MT-13377 to S. Richard).

Submitted: 25 November 2008
Accepted: 24 March 2009

References

Batsché, E., M. Yaniv, and C. Muchardt. 2006. The human SWI/SNF subunit Brm is a regulator of alternative splicing. *Nat. Struct. Mol. Biol.* 13:22–29.

Ben Fredj, N., J. Grange, R. Sadoul, S. Richard, Y. Goldberg, and V. Boyer. 2004. Depolarization-induced translocation of the RNA-binding protein Sam68 to the dendrites of hippocampal neurons. *J. Cell Sci.* 117:1079–1090.

Bentley, D.L. 2005. Rules of engagement: co-transcriptional recruitment of pre-mRNA processing factors. *Curr. Opin. Cell Biol.* 17:251–256.

Bianchini, A., M. Loiarro, P. Bielli, R. Busà, M.P. Paronetto, F. Loreni, R. Geremia, and C. Sette. 2008. Phosphorylation of eIF4E by MNKs supports protein synthesis, cell cycle progression and proliferation in prostate cancer cells. *Carcinogenesis.* 29:2279–2288.

Braun, R.E. 1998. Post-transcriptional control of gene expression during spermatogenesis. *Semin. Cell Dev. Biol.* 9:483–489.

Busà, R., M.P. Paronetto, D. Farini, E. Pierantozzi, F. Botti, D.F. Angelini, F. Attisani, G. Vespasiani, and C. Sette. 2007. The RNA-binding protein Sam68 contributes to proliferation and survival of human prostate cancer cells. *Oncogene.* 26:4372–4382.

Cammas, A., F. Pileur, S. Bonnal, S.M. Lewis, N. Lévêque, M. Holcik, and S. Vagner. 2007. Cytoplasmic relocalization of heterogeneous nuclear ribonucleoprotein A1 controls translation initiation of specific mRNAs. *Mol. Biol. Cell.* 18:5048–5059.

Chawla, G., C.H. Lin, A. Han, L. Shiue, M. Ares, and D.L. Black. 2009. Sam68 regulates a set of alternatively spliced exons during neurogenesis. *Mol. Cell. Biol.* 29:201–213.

Chenard, C.A., and S. Richard. 2008. New implications for the QUAKING RNA binding protein in human disease. *J. Neurosci. Res.* 86:233–242.

Cheng, C., and P.A. Sharp. 2006. Regulation of CD44 alternative splicing by SRm160 and its potential role in tumor cell invasion. *Mol. Cell. Biol.* 26:362–370.

Cheung, N., L.C. Chan, A. Thompson, M.L. Cleary, and C.W. So. 2007. Protein arginine-methyltransferase-dependent oncogenesis. *Nat. Cell Biol.* 9:1208–1215.

Collier, B., B. Gorgoni, C. Loveridge, H.J. Cooke, and N.K. Gray. 2005. The DAZL family proteins are PABP-binding proteins that regulate translation in germ cells. *EMBO J.* 24:2656–2666.

Coyle, J.H., B.W. Guzik, Y.C. Bor, L. Jin, L. Eisner-Smerage, S.J. Taylor, D. Rekosh, and M.L. Hammarskjold. 2003. Sam68 enhances the cytoplasmic utilization of intron-containing RNA and is functionally regulated by the nuclear kinase Sik/BRK. *Mol. Cell. Biol.* 23:92–103.

Elliott, D. 2003. Pathways of post-transcriptional gene regulation in mammalian germ cell development. *Cytogenet. Genome Res.* 103:210–216.

Francis, R., M.K. Barton, J. Kimble, and T. Schedl. 1995. Analysis of the multiple roles of gld-1 in germline development: interactions with the sex determination cascade and the glp-1 signaling pathway. *Genetics.* 139:579–606.

Fumagalli, S., N.F. Totty, J.J. Hsuan, and S.A. Courtneidge. 1994. A target for Src in mitosis. *Nature.* 368:871–874.

Gastwirt, R.F., C.W. McAndrew, and D.J. Donoghue. 2007. Speedy/RINGO regulation of CDKs in cell cycle, checkpoint activation and apoptosis. *Cell Cycle.* 6:1188–1193.

Geremia, R., C. Boitani, M. Conti, and V. Monesi. 1977. RNA synthesis in spermatocytes and spermatids and preservation of meiotic RNA during spermiogenesis in the mouse. *Cell Differ.* 5:343–355.

Grange, J., V. Boyer, R. Fabian-Fine, N.B. Fredj, R. Sadoul, and Y. Goldberg. 2004. Somatodendritic localization and mRNA association of the splicing regulatory protein Sam68 in the hippocampus and cortex. *J. Neurosci. Res.* 75:654–666.

Grivna, S.T., B. Pyhtila, and H. Lin. 2006. MIWI associates with translational machinery and PIWI-interacting RNAs (piRNAs) in regulating spermatogenesis. *Proc. Natl. Acad. Sci. USA.* 103:13415–13420.

Haren, L., M.H. Remy, I. Bazin, I. Callebaut, M. Wright, and A. Merdes. 2006. NEDD1-dependent recruitment of the γ-tubulin ring complex to the centrosome is necessary for centriole duplication and spindle assembly. *J. Cell Biol.* 172:505–515.

Hay, N., and N. Sonenberg. 2004. Upstream and downstream of mTOR. *Genes Dev.* 18:1926–1945.

Hogan, B., R. Beddington, F. Costantini, and E. Lacy. 1994. Manipulating the Mouse Embryo. Cold Spring Harbor Laboratory Press. Cold Spring Harbor, NY. 497 pp.

Iguchi, N., J.V. Tobias, and N.B. Hecht. 2006. Expression profiling reveals meiotic male germ cell mRNAs that are translationally up- and down-regulated. *Proc. Natl. Acad. Sci. USA.* 103:7712–7717.

Kleene, K.C. 2001. A possible meiotic function of the peculiar patterns of gene expression in mammalian spermatogenic cells. *Mech. Dev.* 106:3–23.

Kornblihtt, A.R., M. de la Mata, J.P. Fededa, M.J. Munoz, and G. Nogues. 2004. Multiple links between transcription and splicing. *RNA.* 10:1489–1498.

Kuersten, S., and E.B. Goodwin. 2003. The power of the 3′ UTR: translational control and development. *Nat. Rev. Genet.* 4:626–637.

Lasko, P., P. Cho, F. Poulin, and N. Sonenberg. 2005. Contrasting mechanisms of regulating translation of specific *Drosophila* germline mRNAs at the level of 5′-cap structure binding. *Biochem. Soc. Trans.* 33:1544–1546.

Lee, M.H., and T. Schedl. 2001. Identification of in vivo mRNA targets of GLD-1, a maxi-KH motif containing protein required for *C. elegans* germ cell development. *Genes Dev.* 15:2408–2420.

Li, J., Y. Liu, B.O. Kim, and J.J. He. 2002. Direct participation of Sam68, the 68-kilodalton Src-associated protein in mitosis, in the CRM1-mediated Rev nuclear export pathway. *J. Virol.* 76:8374–8382.

Loiarro, M., F. Capolunghi, N. Fantò, G. Gallo, S. Campo, B. Arseni, R. Carsetti, P. Carminati, R. De Santis, V. Ruggiero, and C. Sette. 2007. Pivotal advance: inhibition of MyD88 dimerization and recruitment of IRAK1 and IRAK4 by a novel peptidomimetic compound. *J. Leukoc. Biol.* 82:801–810.

Lukong, K.E., and S. Richard. 2003. Sam68, the KH domain-containing superSTAR. *Biochim. Biophys. Acta.* 1653:73–86.

Lukong, K.E., K.W. Chang, E.W. Khandjian, and S. Richard. 2008. RNA-binding proteins in human genetic disease. *Trends Genet.* 24:416–425.

Matter, N., P. Herrlich, and H. Konig. 2002. Signal-dependent regulation of splicing via phosphorylation of Sam68. *Nature.* 420:691–695.

McBride, A.E., A. Schlegel, and K. Kirkegaard. 1996. Human protein Sam68 relocalization and interaction with poliovirus RNA polymerase in infected cells. *Proc. Natl. Acad. Sci. USA.* 93:2296–2301.

Michlewski, G., J.R. Sanford, and J.F. Cáceres. 2008. The splicing factor SF2/ASF regulates translation initiation by enhancing phosphorylation of 4E-BP1. *Mol. Cell.* 30:179–189.

Monesi, V. 1964. Ribonucleic acid synthesis during mitosis and meiosis in the mouse testis. *J. Cell Biol.* 22:521–532.

Paronetto, M.P., F. Zalfa, F. Botti, R. Geremia, C. Bagni, and C. Sette. 2006. The nuclear RNA-binding protein Sam68 translocates to the cytoplasm and associates with the polysomes in mouse spermatocytes. *Mol. Biol. Cell.* 17:14–24.

Paronetto, M.P., T. Achsel, A. Massiello, C.E. Chalfant, and C. Sette. 2007. The RNA-binding protein Sam68 modulates the alternative splicing of Bcl-x. *J. Cell Biol.* 176:929–939.

Pyronnet, S., J. Dostie, and N. Sonenberg. 2001. Suppression of cap-dependent translation in mitosis. *Genes Dev.* 15:2083–2093.

Richard, S., N. Torabi, G.V. Franco, G.A. Tremblay, T. Chen, G. Vogel, M. Morel, P. Cleroux, A. Forget-Richard, S. Komarova, et al. 2005. Ablation of the Sam68 RNA binding protein protects mice from age-related bone loss. *PLoS Genet.* 1:e74.

Richard, S., G. Vogel, M.E. Huot, T. Guo, W.J. Muller, and K.E. Lukong. 2008. Sam68 haploinsufficiency delays onset of mammary tumorigenesis and metastasis. *Oncogene.* 27:548–556.

Richter, J.D., and N. Sonenberg. 2005. Regulation of cap-dependent translation by eIF4E inhibitory proteins. *Nature.* 433:477–480.

Rossi, P., F. Lolicato, P. Grimaldi, S. Dolci, A. Di Sauro, D. Filipponi, and R. Geremia. 2008. Transcriptome analysis of differentiating spermatogonia stimulated with kit ligand. *Gene Expr. Patterns.* 8:58–70.

Sanford, J.R., J.D. Ellis, D. Cazalla, and J.F. Cáceres. 2005. Reversible phosphorylation differentially affects nuclear and cytoplasmic functions of splicing factor 2/alternative splicing factor. *Proc. Natl. Acad. Sci. USA.* 102:15042–15047.

Sassone-Corsi, P. 2002. Unique chromatin remodeling and transcriptional regulation in spermatogenesis. *Science.* 296:2176–2178.

Schafer, M., K. Nayernia, W. Engel, and U. Schafer. 1995. Translational control in spermatogenesis. *Dev. Biol.* 172:344–352.

Sette, C., M. Barchi, A. Bianchini, M. Conti, P. Rossi, and R. Geremia. 1999. Activation of the mitogen-activated protein kinase ERK1 during meiotic progression of mouse pachytene spermatocytes. *J. Biol. Chem.* 274:33571–33579.

Sette, C., M.P. Paronetto, M. Barchi, A. Bevilacqua, R. Geremia, and P. Rossi. 2002. Tr-kit-induced resumption of the cell cycle in mouse eggs requires activation of a Src-like kinase. *EMBO J.* 21:5386–5395.

Taylor, S.J., and D. Shalloway. 1994. An RNA-binding protein associated with Src through its SH2 and SH3 domains in mitosis. *Nature.* 368:867–871.

Tisserant, A., and H. König. 2008. Signal-regulated Pre-mRNA occupancy by the general splicing factor U2AF. *PLoS ONE.* 3:e1418.

Turner, J.M., S.K. Mahadevaiah, O. Fernandez-Capetillo, A. Nussenzweig, X. Xu, C.X. Deng, and P.S. Burgoyne. 2005. Silencing of unsynapsed meiotic chromosomes in the mouse. *Nat. Genet.* 37:41–47.

Venables, J.P., and I. Eperon. 1999. The roles of RNA-binding proteins in spermatogenesis and male infertility. *Curr. Opin. Genet. Dev.* 9:346–354.

Volk, T., D. Israeli, R. Nir, and H. Toledano-Katchalski. 2008. Tissue development and RNA control: "HOW" is it coordinated? *Trends Genet.* 24:94–101.

Walker, W.H., F.J. Delfino, and J.F. Habener. 1999. RNA processing and the control of spermatogenesis. *Front. Horm. Res.* 25:34–58.

Wang, L.L., S. Richard, and A.S. Shaw. 1995. P62 association with RNA is regulated by tyrosine phosphorylation. *J. Biol. Chem.* 270:2010–2013.

Wiltshire, T., C. Park, K.A. Caldwell, and M.A. Handel. 1995. Induced premature G2/M-phase transition in pachytene spermatocytes includes events unique to meiosis. *Dev. Biol.* 169:557–567.

Zhang, Z., I. Kostetskii, W. Tang, L. Haig-Ladewig, R. Sapiro, Z. Wei, A.M. Patel, J. Bennett, G.L. Gerton, S.B. Moss, et al. 2006. Deficiency of SPAG16L causes male infertility associated with impaired sperm motility. *Biol. Reprod.* 74:751–759.